

Performance of Fixed Speed Wind Turbines under System Frequency Deviations

Andreas Sumper^{*,†}
Oriol Gomis-Bellmunt^{*,†}
Antoni Sudrià-Andreu^{*,†}
Roberto Villafáfila-Robles^{*}
Joan Rull-Duran^{*}

* Centre d'Innovació Tecnològica en Convertidors Estàtics i Accionaments (CITCEA-UPC),

Departament d'Enginyeria Elèctrica, Universitat Politècnica de Catalunya.
EU d'Enginyeria Tècnica Industrial de Barcelona, Comte d'Urgell, 187

08036 Barcelona, Spain

Phone: +34 (93) 413-7432

Fax: +34 (93) 401-7433

Email: sumper@citcea.upc.edu

URL: <http://www.citcea.upc.edu>

† Catalonia Institute for Energy Research (IREC)

Abstract

This paper studies the impact of system frequency deviations on the operation of fixed speed induction generators used in wind turbine generation systems (WTGS). It presents an analytic method to predict the angular speed, torque and current during and after a frequency disturbance. The proposed method can be used to evaluate the operation limits of the WTGS during frequency deviations.

1 Introduction

Several authors have treated the impact of voltage dips on fixed speed and variable speed WTGS and analyzed voltage and transient stability during those events [2–5].

Literature reports the impact of WTGS on the system frequency [6], inertia response of different wind turbine technologies [7] and comparison between inertia response of single fed and double fed induction generators [8]. WTGS can also have control strategies for system frequency regulation

[9–11].

During a frequency variations, the operation point of wind turbine is changed due to the modification of the machine reactances and the slip. To prevent inappropriate operation of wind parks, they are equipped with a frequency relay that disconnects it after a severe frequency disturbance [12]. In power systems with high wind power penetration, those frequency deviations can provoke a massive wind farms disconnection that can lead to power system oscillations [13]. Modern WTGS usually are variable speed WTGS. Nevertheless, fixed speed WTGS were installed in large proportions in power grids over the last years. Therefore it is still a matter of interest to study the interaction of fixed speed WTGS with power system during frequency deviations.

This work presents an analytic method for the calculation of angular speed, torque and current for WTGS before, during and after a frequency disturbance. In literature, [15] treats a small-signal dynamic model of a fixed-speed (induction machine based) wind farm connected to an electrical power

system and [16] introduces a dynamic induction machine model representations for frequency variations. Both authors are not treating the impact of frequency deviations on the operation point of the WTGS.

2 Linearized WTGS Equations

In order to analyze the impact of frequency deviations on the operation point of WTGS, the torque-angular speed characteristics (Fig. 1) of a squirrel cage induction generator (SCIG) and the wind turbine rotor torque-angular speed characteristic should be studied. The stable operation point of a fixed speed WTGS is the intersection of both torque curves at any system frequency. The SCIG torque characteristics can be linearized by the approach from Kloss [23].

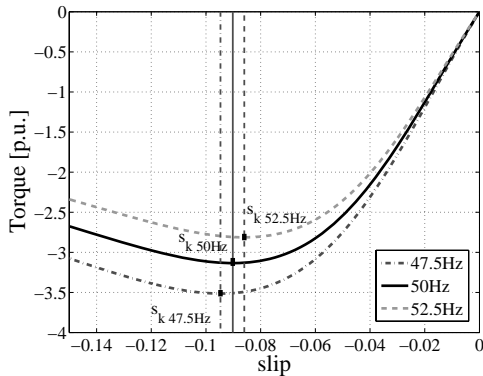


Figure 1: Torque-slip characteristic of an induction machine with different system frequencies

2.1 Turbine rotor torque

The aerodynamic turbine rotor model expressed in [18] and [20] is used in order to describe the turbine rotor torque generated from the wind.

Assuming a constant average wind speed, wind turbines operate around a steady-state operating point. For small disturbances, torque equation can be linearized over this steady-state operation point

[15] by

$$\Delta T_M = K_\alpha \Delta \omega_M + K_\beta \Delta v_w + K_\gamma \Delta \vartheta \quad (1)$$

where T_{M0} and ω_{M0} are the mechanical torque and the angular speed at the operation point and

$$K_\alpha = \frac{1}{\omega_{M0}} (K_a - T_{M0})$$

$$K_\beta = \frac{1}{\omega_{M0}} K_b$$

$$K_\gamma = \frac{1}{\omega_{M0}} K_c$$

being

$$K_a = \left. \frac{\partial P_w}{\partial \omega_M} \right|_{\lambda_0, \vartheta_0}$$

$$K_b = \left. \frac{\partial P_w}{\partial v_w} \right|_{\lambda_0, \vartheta_0}$$

$$K_c = \left. \frac{\partial P_w}{\partial \vartheta} \right|_{\lambda_0, \vartheta_0}$$

2.2 Steady State operation point after a frequency disturbance

Fig. 2 shows the torque-speed characteristics of both induction generator and turbine rotor. A modification of the system frequency will modify the generator torque, defined by approximation by Kloss. The former stable operation point T_{m0} and ω_{m0} will be modified and the new stable operation point T_{m1} and ω_{m1} is established. Assuming constant wind speed and no fast active stall control reaction, the rotor torque increment expressed in p.u. and referred to the high speed shaft:

$$\Delta T = K_\alpha \Delta \omega_m = K_\alpha (\omega_{m1} - \omega_{m0}) \quad (2)$$

where

$$K_\alpha = \frac{1}{\omega_{M0}} \left(\frac{1}{2} \rho R^3 v_{w0} \left. \frac{\partial C_p}{\partial \lambda} \right|_{\lambda_0, \vartheta_0} - T_{M0} \right) \quad (3)$$

In order to be able to equal machine and turbine rotor torque equations, (3) should be converted to p.u. system. The new operation steady state torque after a frequency disturbance is yielded setting equal both equations. Therefore,

$$T_{m0} + K_\alpha \Delta\omega = 2 \frac{T_k}{s_k} \left(1 - \frac{\omega_{m0} + \Delta\omega}{\omega_e}\right) \quad (4)$$

The angular speed after the frequency disturbance is:

$$\Delta\omega = \frac{-T_{m0} + 2 \frac{T_k}{s_k} - 2 \frac{T_k}{s_k} \frac{\omega_{m0}}{\omega_e}}{K_\alpha + 2 \frac{T_k}{s_k \omega_e}} \quad (5)$$

The generator torque T_{m1} can be yield then by Kloss torque equation.

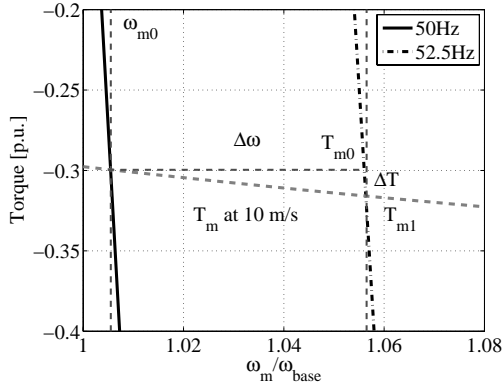


Figure 2: New operation point after a frequency disturbance

2.3 Torque and speed variations during a frequency slope

In this work frequency variation will be linearized by using frequency slopes during the disturbance period in order to allow an analytical approach. During the frequency slope with a constant $\frac{df}{dt}$ for each operation point, angular speed and torque can be yield by (5). The final torque equation during a frequency slope is expressed by

$$T_e = T_{m0} - 2H\dot{\omega} + K_\alpha\dot{\omega}(t - t_0) \quad (6)$$

For $t_0 = 0$, the torque can be expressed by

$$T_e = T_{m0} - 2H\dot{\omega} + K_\alpha\dot{\omega}t \quad (7)$$

2.4 Calculation of the generator current

The generator current can be expressed by

$$I_s = \sqrt{(T_{m0} - 2H\dot{\omega} + K_\alpha\dot{\omega}t) \frac{\left(\frac{R'_r}{s}\right)^2 + \left(\frac{\omega_e}{\omega_b}\right)^2 (X_m - X_r)^2}{\frac{\omega_e}{\omega_b} X_m^2 \frac{R'_r}{s}}} \quad (8)$$

3 Validation of the linear approximation approach through Computer Simulations

To show that the proposed analytic method can be used for the analysis of real installations, simulation tool for power systems DigSILENT PowerFactory was used to validate the analytic results. DigSILENT PowerFactory is a well known simulation program for wind generators and power systems [25].

A fixed speed WTGS was modeled. The shaft is modeled as a two mass system and a 3th order induction generator model [26] was used to represent the speed variation with sufficient accuracy. An external grid equivalent model [27] was used. Frequency is modified by the increase of the synchronous machine speed of the equivalent grid model.

Fig. 3(a), Fig. 3(b) and Fig. 3(c) compares the generator torque, current and angular speed of the analytic method with the digital simulation results. It can be seen, that for the frequency slope and the steady state value after the frequency change, the shape and the values of torque, current and speed curve match almost well. Both simulations of torque and current show transients at the begin and end of the frequency slope that are related to the shaft stiffness and damping constants. Those

transients can not be predicted with the proposed analytic model.

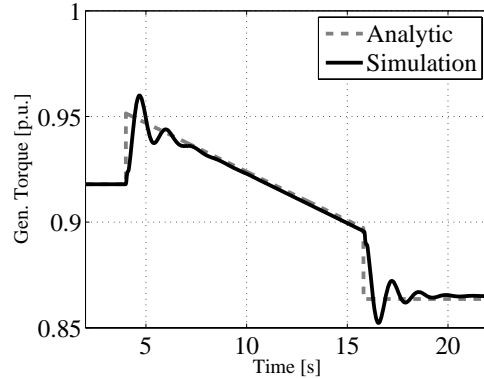
4 Discussion of the results and conclusion

This work tackles an analytical approach to predict the angular speed, torque and current of fixed speed WTGS before, during and after frequency deviations. It can be seen, that for frequency decreases, the limiting factor is the value of the slope $\frac{d\omega}{dt}$ and the inertia of the WTGS. For frequency increases, the current is limited by the steady state current after the frequency disturbance. The angular speed of the WTGS generally is limited by an over-speed protection device, which will be activated if the limit will be exceeded.

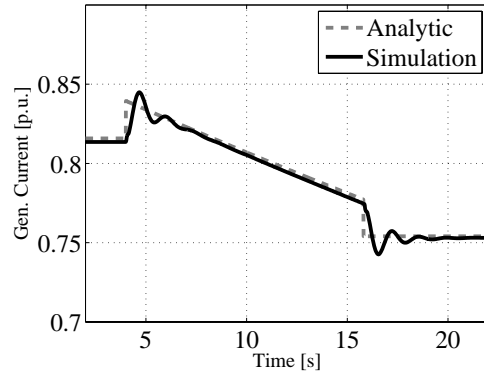
As the presented method is analytic, the transients at the beginning and at the end of the frequency disturbance can not be predicted. Those transients occur due to the stiffness and damping of the shaft. Such oscillations are found by digital simulation.

References

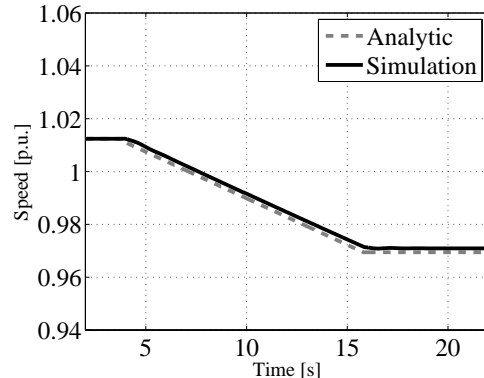
- [1] R. Villafafila, A. Sumper, A. Suwannarat, B. Bak-Jensen, R. Ramirez, and A. Sudria. On wind power integration into electrical power system: Spain vs: Denmark. In *International Conference on Renewable Energies and Power Quality (ICREPQ)*, 2007.
- [2] N. R. Ullah, T. Thiringer, and D. Karlsson. Voltage and transient stability support by wind farms complying with the e.on netz grid code. *IEEE Transactions on Power Systems*, 22(4):1647–1656, 2007.
- [3] S. Seman, J. Niiranen, and A. Arkkio. Ride-through analysis of doubly fed induction wind-power generator under unsymmetrical network disturbance. *IEEE Transactions on Power Systems*, 21(4):1782–1789, Nov. 2006.
- [4] Adrià Junyent-Ferré, Andreas Sumper, Oriol Gomis-Bellmunt, Marc Sala, and Montserrat Mata. Digital simulation of voltage dip characteristics of wind turbine systems. In *9th Inter-*



(a) Torque during a frequency disturbance from 50 Hz to 48 Hz.



(b) Generator current during a frequency disturbance from 50 Hz to 48 Hz.



(c) Generator angular speed during a frequency disturbance from 50 Hz to 48 Hz.

Figure 3: Comparison of the results (i) of the analytic calculation method torque presented in (7); and (ii) results obtained by digital simulation using DigSILENT PowerFactory simulation tool.

- national Conference on Electrical Power Quality and Utilization*, 2007.
- [5] A.I. Estanqueiro. A dynamic wind generation model for power systems studies. *IEEE Transactions on Power Systems*, 22(3):920–928, 2007.
- [6] R.G. de Almeida and J.A.P. Lopes. Participation of doubly fed induction wind generators in system frequency regulation. *IEEE Transactions on Power Systems*, 22(3):944–950, 2007.
- [7] G. Lalor, A. Mullane, and M. O’Malley. Frequency control and wind turbine technologies. *IEEE Transactions on Power Systems*, 20(4):1905–1913, 2005.
- [8] A. Mullane and M. O’Malley. The inertial response of induction-machine-based wind turbines. *IEEE Transactions on Power Systems*, 20(3):1496–1503, Aug. 2005.
- [9] Y. G. Rebours, D. S. Kirschen, M. Trotignon, and S. Rossignol. A survey of frequency and voltage control ancillary services; part i: Technical features. *IEEE Transactions on Power Systems*, 22(1):350–357, 2007.
- [10] Y. G. Rebours, D. S. Kirschen, M. Trotignon, and S. Rossignol. A survey of frequency and voltage control ancillary services; part ii: Economic features. *IEEE Transactions on Power Systems*, 22(1):358–366, 2007.
- [11] J. Matevosyan, T. Ackermann, and S. M. Bolk. *Wind Power in Power Systems*, chapter Technical Regulations for the Interconnection of Wind Farms to the Power System, pages 115–142. Wiley, 2005.
- [12] T. Adrada-Guerra, J. Amador-Guerra, and J. Moreno-Mohino. *Sistemas Eolicos de Producción de Energía Eléctrica (in spanish)*, chapter Instalaciones eléctricas de los parques eólicos, pages 300–328. Rueda, 2003.
- [13] A. Causebrook, D.J. Atkinson, and A.G. Jack. Fault ride-through of large wind farms using series dynamic braking resistors (march 2007). *IEEE Transactions on Power Systems*, 22(3):966–975, 2007.
- [14] Gerard A. Maas. Interim report: System disturbance on 4 november 2006. Technical report, Union for the Co-ordination of Transmission of Electricity (UCTE), 2006.
- [15] A. Tabesh and R. Iravani. Small-signal dynamic model and analysis of a fixed-speed wind farm - a frequency response approach. *IEEE Transactions on Power Delivery*, 21(2):778–787, 2006.
- [16] T. Thiringer and J. Luomi. Comparison of reduced-order dynamic models of induction machines. *IEEE Transactions on Power Systems*, 16(1):119–126, 2001.
- [17] S. Heier. *Grid Integration of Wind Energy Conversion Systems*. John Wiley and Sons, 1998.
- [18] J. G. Slootweg. *Wind Power in Power Systems*, chapter Reduced-order Modelling of Wind Turbines, pages 555–585. Wiley, 2005.
- [19] J.L. Rodríguez-Amenedo and J. Sanz-Feito. *Sistemas Eolicos de Producción de Energía Eléctrica (in spanish)*, chapter Tecnologia de Aerogeneradores, pages 98–179. Rueda, 2003.
- [20] Vladislav Akhmatov. *Analysis of Dynamic Behaviour of Electric Power Systems with Large Amount of Wind Power*. PhD thesis, Technical University of Denmark, 2003.
- [21] V. Akhmatov, H. Knudsen, and H. Knudsen. Advanced simulation of windmills in the electric power supply. *Electric Power and Energy Systems*, 22(6):421–434, 2000.
- [22] Paul C. Krause. *Analysis of electric machinery*. McGraw-Hill, 1986.
- [23] Rolf Fischer. *Elektrische Maschinen (in german)*. Carl Hanser Verlag, München, Wien, 1979.
- [24] Pablo Ledesma. *Análisis dinámico de sistemas eléctricos con generación eólica (in spanish)*. PhD thesis, Universidad Carlos III de Madrid, 2001.
- [25] M.A. Poller. Doubly-fed induction machine models for stability assessment of wind farms. In *Proc. IEEE Bologna Power Tech*, volume 3, pages 6 pp. Vol.3–, 2003.

- [26] Vlaslav Akhmatov. *Induction Generators for Wind Power*. Multi-Science Publishing Company, Ltd, 2005.
- [27] AEE. Procedimiento de verificación, validación y certificación de los requisitos del po 12.3 sobre la prespuesta de las instalaciones eólicas ante huecos de tensión. Technical report, Asociación Empresarial Eólica, 2007. Draft, 2007.